Ind. J. Pharm. Edu. Res., 2024; 58(4s):s1271-s1281.
https://www.ijper.org

Original Article

An Albumin-Based Amygdalin-Glutaraldehyde Nanoparticle Induces Apoptosis in Oral Cancer KB Cells

Murugan Alwarkurichi Munusamy[1,*], Kalpana Sukumar[2], Muruganantham Bharathi[3], Abdullah A. Alarfaj[4], Samer Hasan Hussein-Al-Ali[5]

[1]Department of Chemistry, Saveetha School of Engineering, Saveetha Institute of Medical and Technical Sciences (SIMATS), Saveetha University, Chennai, Tamil Nadu, INDIA.
[2]Department of Physics, Saveetha Engineering College, Saveetha Nagar, Thandalam, Chennai, Tamil Nadu, INDIA.
[3]Department of Biochemistry, Centre for Drug Discovery, Karpagam Academy of Higher Education, Coimbatore, Tamil Nadu, INDIA.
[4]Department of Botany and Microbiology, College of Science, King Saud University, Riyadh, SAUDI ARABIA.
[5]Department of Chemistry, Faculty of Sciences, Isra University, Amman, JORDAN.

ABSTRACT

Background: There is potential for nanotechnology to address the drawbacks associated with conventional cancer therapies. The current study was undertaken to formulate amygdalin-functionalized Albumin-Glutaraldehyde Nanoparticles (AAG-NPs) and evaluate their antimicrobial and anticancer properties against oral cancer KB cells. **Materials and Methods:** The AAG-NPs were synthesized and characterized using UV-visible spectroscopy, XRD, SEM, TEM, DLS, FT-IR and PL analyses. The well diffusion technique was used to examine the antimicrobial potentials of the AAG-NPs against various pathogens like *S. pneumoniae, B. megaterium, B. subtilis, P. aeruginosa, P. vulgaris, V. cholerae*, and *C. albicans*. The cytotoxicity of AAG-NPs was assessed by MTT assay at various concentrations. Fluorescent staining tests were performed on KB cells treated with AAG-NPs to assess apoptosis. The levels of pro- and anti-apoptotic protein expressions were analyzed using assay kits. **Results:** The various characterization analyses demonstrated the presence of spherical-shaped AAG-NPs with an average particle size of 148.30 nm. The occurrence of various elements and functional groups in AAG-NPs was also observed. The synthesized AAG-NPs showed excellent antimicrobial activities by effectively inhibiting the growth of various pathogens. The treatment of AAG-NPs significantly inhibited the growth of KB cells. As a result of fluorescent staining assays, NP-treated KB cells showed evidence of apoptosis. The AAG-NPs treatment increased apoptotic protein expression in KB cells. **Conclusion:** The current results demonstrate that AAG-NPs inhibit cellular proliferation and induce apoptosis in KB cells. Nevertheless, further study is necessary to understand the molecular mechanisms underlying AAG-NPs-induced apoptosis in KB cells.

Keywords: Amygdalin, Oral cancer, Albumin, Apoptosis, KB cells.

Correspondence:
Dr. Murugan Alwarkurichi Munusamy
Department of Chemistry, Saveetha School of Engineering, Saveetha Institute of Medical and Technical Sciences (SIMATS), Saveetha University, Chennai-602105, Tamil Nadu, INDIA.
Email: ammurugan11@gmail.com

Received: 28-05-2024;
Revised: 30-07-2024;
Accepted: 07-10-2024.

INTRODUCTION

Oral Cancer (OC) is a specific type of head and neck cancer that mostly affects the oral cavity and oropharynx. The condition is distinguished by the existence of cancerous growths in different tissues, such as the lips, tongue, palate and gingiva.[1] Oral Squamous Cell Carcinoma (OSCC) is the major type of oral cancer, making up 90% of all incidences of oral cancer and being one of the top 15 most frequently diagnosed cancers globally. OSCC poses a significant risk due to the high malignancy, death rate and poor prognosis. The treatment of OSCC poses significant challenges because of its elevated recurrence rate and metastasis to the lymph node.[2] Possible risk factors for oral cancer include heavy alcohol and tobacco consumption, oral hygiene issues, betel chewing and dietary deficiencies. Individuals diagnosed with oral cancer may exhibit initial signs that include non-healing ulcers, bleeding within the mouth, leukoplakia and anomalous masses in the oral cavity.[3] Nevertheless, in the initial phases of oral cancer, a significant number of individuals may not manifest evident symptoms or very few signs, which lead to a late diagnosis and, in certain cases, can lead to the disease advancing to a late stage that cannot be cured, ultimately resulting in high medical costs and even death.[4]

Surgery is the standard treatment for early-stage OSCC patients, as it can completely eradicate the tumors. The primary treatments for patients in the developed stage include radiation, chemotherapy, immunotherapy and combination therapy.[5] Despite significant optimization of these therapies in recent

DOI: 10.5530/ijper.58.4s.122

decades, their therapeutic efficacy remains suboptimal, resulting in an overall 5-year survival rate of less than 60%.[6] Research suggests that a primary reason for the limited effectiveness of treatment is the low efficiency of the Drug Delivery System (DDS), which leads to insufficient levels of antitumor drugs at the cancer site, hence reducing their ability to combat cancer. Thus, significant efforts have been made to develop new DDSs that can enhance the drug concentration at the tumor site.[7] The NPs used as DDSs can potentially decrease drug toxicity, improve safety and increase drug specificity. These NPs hold great promise for treating OSCC.[8]

Researchers are currently shifting their attention towards phytochemicals as a potential treatment for cancer, as many standard chemotherapy drugs are derived from plants.[9] The use of phytochemicals in cancer treatment can overcome the limitations of traditional chemotherapeutic drugs, resulting in more effective cancer treatment.[10] Even though combination therapy has advantages over monotherapy, clinical results are still low because of factors such as low bioavailability, poor aqueous solubility, drug durations at the desired site and the lack of drug targeting.[11] Nanotechnology offers innovative nanocarriers that deliver phytochemicals and conventional chemotherapeutic drugs to achieve the most favorable clinical results in cancer treatment.[12] These new carriers have a size range of 1 to 1000 nm and result in enhanced treatment effectiveness and decreased negative effects linked to targeted drugs. These carriers demonstrate their promise through various beneficial characteristics such as enhanced solubility, fewer adverse effects, increased effectiveness, improved dose frequency, decreased drug resistance, targeted drug delivery, enhanced bioavailability and improved patient compliance.[13]

Amygdalin is a disaccharide that occurs naturally in large concentrations in the fruit kernels of Rosaceae species, such as bitter almonds, peaches and apricots and is reported to possess several pharmacological properties. Several earlier studies already highlighted that amygdalin exhibited anticancer,[14] anti-inflammatory and antioxidant,[15] immunomodulatory,[16] antibacterial[17] and anti-renal fibrosis[18] activities. Therefore, the current study was undertaken to formulate the amygdalin-functionalized Albumin-Glutaraldehyde Nanoparticles (AAG-NPs) and evaluate their anticancer properties against oral cancer KB cells.

MATERIALS AND METHODS

Chemicals

The chemicals and reagents used in this work, including amygdalin, albumin and glutaraldehyde, were purchased from Sigma-Aldrich, USA. The ELISA-based assay kits for biochemical assays were procured from Elabscience, USA and R&D Systems, USA, respectively.

Preparation of AAG-NPs

To synthesize the AAG-NPs, 20 mg of amygdalin was initially mixed with 4 mL of an ethanol solution. Subsequently, a suspension containing 200 mg of albumin was completely dissolved in Milli-Q water (1 mL). The albumin solution was constantly stirred at 500 rpm at 37°C and the amygdalin solution was mixed slowly and continuously. Following 2 hr a 30 µL of 25% glutaraldehyde was introduced as a cross-linking agent. The suspension was subsequently agitated for 24 hr. After 24 hr the NPs were purified by centrifuging for 15 min at 30,000×g. The obtained AAG-NPs were placed on the freeze dryer (Zirbus Vaco 5, Germany) and subjected to a freeze-drying process for 24 hr at -50°C, following a pre-freezing period of 24 hr at -70°C. The resultant NPs were then used for characterization and biological assays.

Characterization of the synthesized AAG-NPs

The synthesis of AAG-NPs was analyzed using UV-visible spectroscopy. The formation of AAG-NPs was observed and the light absorption at different wavelengths between 200 and 1000 nm was analyzed using a UV-visible spectrophotometer. The AAG-NPs were examined for their crystalline nature using an X-ray Diffractometer (XRD) (PANalytical, X'Pert Pro, USA) with Cu-Kα radiation at a wavelength of λ=0.1541 nm. The scan range was set from 2θ=10-80°. The morphology and elemental compositions of the synthesized AAG-NPs were evaluated using a Scanning Electron Microscope (SEM) and energy-dispersive X-ray spectroscopy (EDAX), respectively. The SEM and EDAX studies were done using a FEI-Nova NanoSEM 450 (Thermofisher, USA) SEM analyzer. The TEM (PHILIPS CM300, Cambridge, USA) was used to analyze the average size and appearance of the AAG-NPs. The copper grid containing the AAG-NPs sample was illuminated using electromagnetic radiation in a vacuum environment. The microphotographs were taken by using an electron beam to scan the material. The distribution patterns and particle size of the synthesized AAG-NPs were analyzed using the Zeta sizer (Nano-Sight NS500, UK) equipment. The FT-IR technique was employed to investigate the functional groups, bonding and stretching of the synthesized AAG-NPs. The AAG-NPs were analyzed using a PerkinElmer Frontier (USA) spectrometer. A spectral analysis was conducted using a KBr disc, covering a range of 4000-500 cm^{-1}. The Photoluminescence (PL) spectrum of the AAG-NPs was recorded using a Perkin Elmer-LS 14 spectrometer.

Antimicrobial activity

The antimicrobial effects of the synthesized AAG-NPs were investigated using the well diffusion technique. The bacterial and fungal pathogens, namely *Streptococcus pneumoniae, Pseudomonas aeruginosa, Bacillus megaterium, Proteus vulgaris, Bacillus subtilis, Vibrio cholerae*, and *Candida albicans* were inoculated onto their respective agar medium and then wells

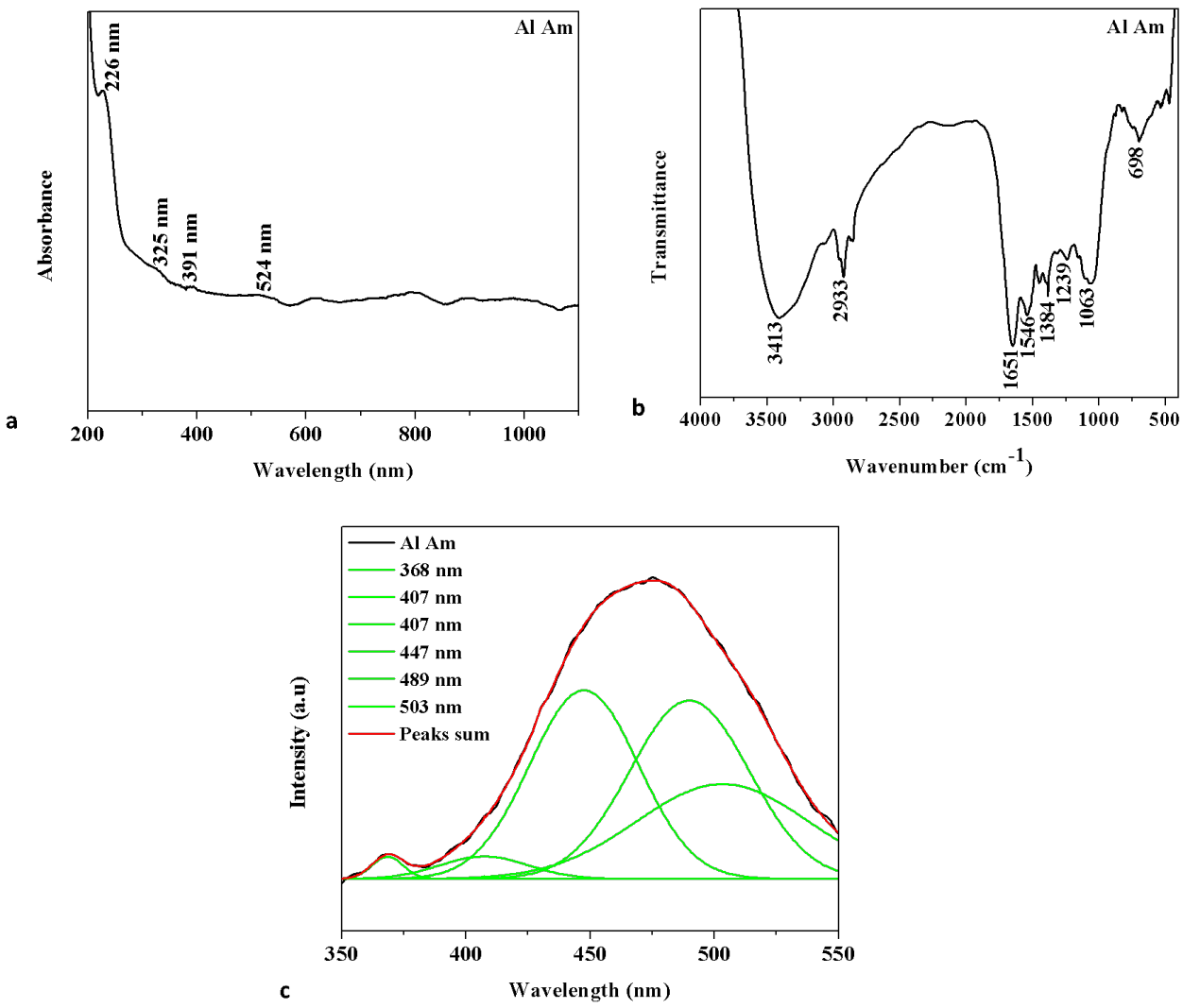

Figure 1: UV-visible spectroscopy, FT-IR and PL analysis of the synthesized AAG-NPs. The absorbance was taken at 200 to 1000 nm wavelengths and the maximum absorbance peak was observed at 226, 325, 391 and 524 nm, respectively (a). The presence of several distinct peaks in the FTIR spectra demonstrates the presence of various functional groups in the synthesized AAG-NPs (b). The PL spectrum of the synthesized AAG-NPs displayed distinct peaks in their emission spectrum at various wavelengths of 368 nm, 407 nm, 407 nm, 447 nm, 489 nm and 503 nm (c).

were made on the agar plate surface at 6 mm diameter using a sterile cork borer. The AAG-NPs samples were loaded onto the wells at different dosages (1, 1.5 and 2 µg) and incubated for 24 hr. After incubation, the plates were evaluated and the zones of inhibition were recorded.

MTT assay

The anti-proliferative activity of AAG-NPs was assessed using the MTT assay. Oral cancer KB cells were loaded separately in the 96-well plate and grown for 24 hr. Following a 24 hr incubation, the cells were treated with different doses of AAG-NPs (1, 5, 10, 25, 50, 100 and 200 µg/mL) for 24 hr. Following incubation, the medium was discarded and then 100 µL of MTT (0.5 mg/mL) was mixed for 4 hr. Subsequently, the MTT reagent was discarded and DMSO (100 µL) was introduced into each well to facilitate the dissolution of the formazan deposits. The measurement of absorbance was conducted using an ELISA reader at a wavelength of 450 nm.

Dual staining

Apoptotic cell death was studied by a dual staining assay on both AAG-NPs-treated and control KB cells. The KB cells were cultivated on a 24-well plate and exposed to IC_{50} concentrations of the synthesized AAG-NPs and 10 µM of doxorubicin as a standard drug for 24 hr. Later, 100 µg/mL of AO/EtBr dye mixture was introduced into the wells for 5 min in a dark place. Finally, the stained cells were analyzed using a fluorescence microscope to detect the presence of apoptosis.

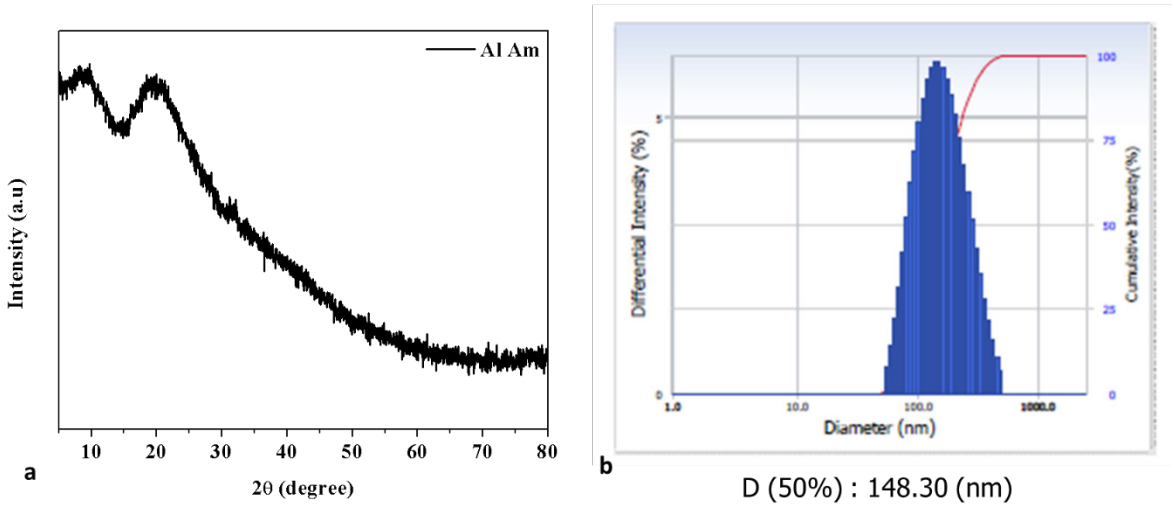

Figure 2: XRD (a) and DLS (b) analyses of the synthesized AAG-NPs. The analysis of the XRD patterns indicates that the AAG-NPs have a cubic crystal structure, with various clear peaks detected at 2θ values. The analysis demonstrates a relative agglomeration with an average hydrodynamic diameter of 148.30 nm.

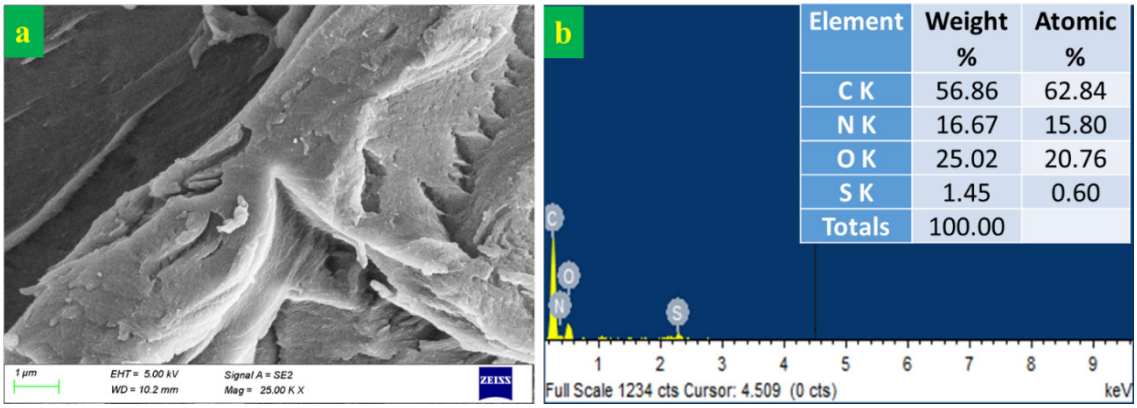

Figure 3: SEM and EDAX analyses of the synthesized AAG-NPs. The microphotographs of (3a) clearly show that the AAG-NPs display hexagonal structures with an aggregated appearance. An EDAX spectrum revealed the primary elements present in the AAG-NPs were 56.86% of Copper (C), 16.67% of Nitrogen (N), 25.02% of Oxygen (O) and 1.45% of Sulfur (S).

DAPI staining

The DAPI staining method was used to investigate the apoptotic cell nuclear morphology of both AAG-NPs-treated and control KB cells. Following the 24 hr growth of KB cells into a 24-well plate, they were treated with IC_{50} concentrations of AAG-NPs and 10 µM of doxorubicin as a standard drug for 24 hr. After a 30 min fixation in a 4% paraformaldehyde solution, the cells were stained with a DAPI stain at a 200 µg/mL concentration for 15 min. Subsequently, the effect of AAG-NPs on nuclear damage and apoptosis in KB cells was investigated using a fluorescence microscope.

Analysis of apoptotic protein expressions

The Bax, Bcl-2, Cyt-C, caspase-3, -8, -9 and p53 expressions were quantified in the cell lysates of both AAG-NPs-treated and control KB cells. The assays were done in triplicate using assay kits and the assays were done using the instructions provided by the manufacturer (Thermo Fisher Scientific, USA).

Statistical analysis

The GraphPad Prism was utilized to analyze the data and the results are reported as a mean±SD of triplicates (n=3). The data were studied using one-way ANOVA and Duncan's Multiple Range Test (DMRT), with a significance level fixed at $p<0.05$.

RESULTS AND DISCUSSION

Nanomaterials play a crucial role in the development of novel and potential treatments for oral cancer. They can be employed as direct antitumor drugs or to develop nano-DDSs for the delivery of anticancer drugs.[19,20] Targeted DDSs have been developed to efficiently deliver anticancer drugs specifically to tumors.[21] Particularly, many types of nanomaterials, including dendrimers,

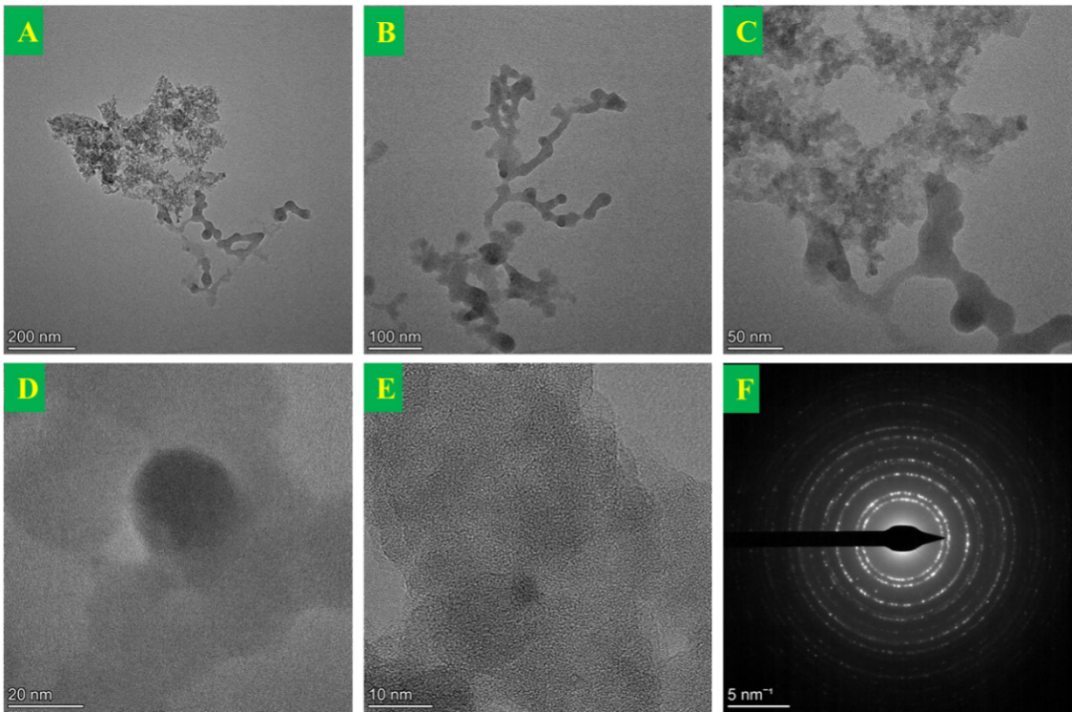

Figure 4: TEM and SAED analyses of the synthesized AAG-NPs. TEM images revealed the presence of spherical-shaped AAG-NPs with significant aggregation (Figure 4A-E). The observed SAED patterns confirmed the crystallization of the AAG-NPs (Figure 4F).

micelles and inorganic NPs, have been extensively studied for their ability to deliver drugs directly to tumors.[22] Nanocarriers offer a promising option for delivering drugs specifically to cancer sites due to their ability to target specific sites, biodegradability, reduced side effects and enhanced stability.[23] Drug carriers can be employed to improve the effectiveness of drugs. Drug carriers alleviate adverse effects by specifically targeting tumors.[24]

Albumin, a pivotal nutritional resource for the body, has been widely studied as a natural vehicle for drug delivery because of its various benefits, including biocompatibility, facile surface modification and excellent biodegradability.[25] Significantly, albumin can naturally incorporate hydrophobic anticancer medicines into its hydrophobic regions, thereby enhancing the pharmacokinetic characteristics and prolonging the circulation time of drugs for targeted delivery to tumors.[26] Furthermore, albumin-bound drug designs effectively accumulate in cancers through the EPR effect, which is characterized by heightened vascular permeability and reduced lymphatic drainage in the macromolecular complex.[27] The present study was conducted to synthesize and characterize the AAG-NPs and evaluate their anticancer potential against oral cancer KB cells.

The formation of AAG-NPs was studied using UV-vis spectrophotometric analysis. The absorbance was conducted at 200 to 1000 nm wavelengths. The findings showed that the absorbance peak with the maximum intensity was observed at 226, 325, 391 and 524 nm, indicating the presence of AAG-NPs (Figure 1a). The FT-IR spectra demonstrate the occurrence of various functional groups in the synthesized AAG-NPs (Figure 1b). Amygdalin exhibits functional properties that are characterized by the presence of an asymmetric and symmetric peak at 2933 cm^{-1}, which is due to the C-H group. The albumin exhibited distinctive peaks at a wavelength of 3413 cm^{-1}, corresponding to the O-H functional group involved in hydrogen bonding. The acetyl CO stretching peaks were seen at 1651 cm^{-1} and 1546 cm^{-1}, respectively. An angular deformation peak with CH_3 symmetry was detected at a wavenumber of 1384 cm^{-1}. The stretching band modes of the metal oxide were observed at frequencies of 1239, 1063 and 698 cm^{-1}, respectively (Figure 1b). The presence of intermolecular hydrogen bonds between the albumins, glutaraldehyde and amygdalin surface matrices in the AAG-NPs is confirmed by the observed peaks. Figure 1c displays the PL spectrum of the synthesized AAG-NPs. The AAG-NPs display distinct peaks in their emission spectrum at wavelengths of 368, 407, 407, 447, 489 and 503 nm.

Figure 2a demonstrates the XRD patterns of the AAG-NPs. The analysis of the XRD patterns indicates that the AAG-NPs have a cubic crystal structure, with various clear peaks detected at 2θ values. The observed peak positions correspond to the crystallographic planes of the NP structure. Thus, it supported the crystalline nature of the synthesized AAG-NPs. The DLS study was conducted to evaluate the hydrodynamic size of the synthesized AAG-NPs (Figure 2b).

The analysis demonstrates a relative agglomeration with an average hydrodynamic diameter of 148.30 nm. In addition, the

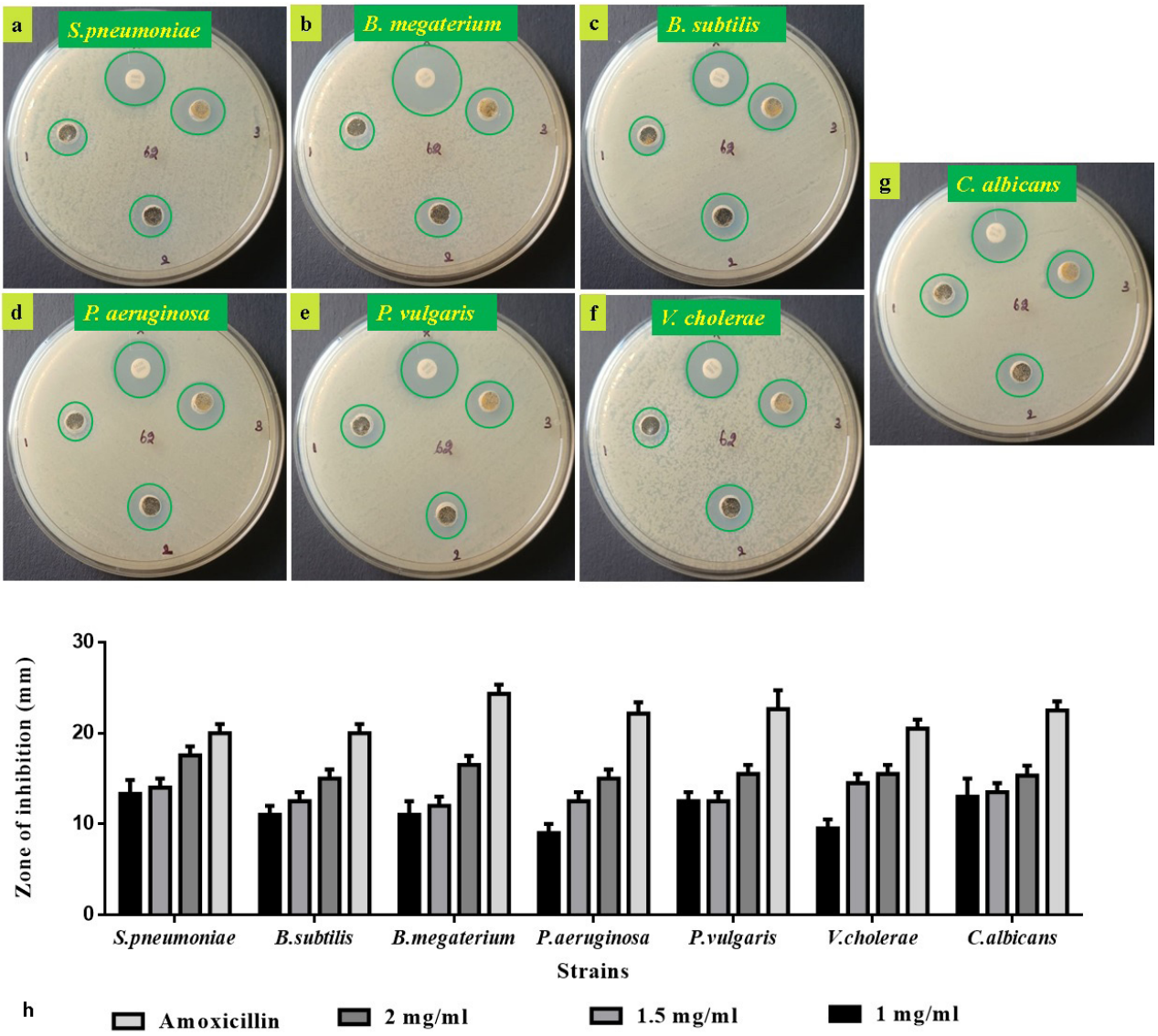

Figure 5: Antimicrobial activity of the synthesized AAG-NPs. The well diffusion technique was used to assess the antimicrobial properties of AAG-NPs. *S. pneumoniae (a), B. megaterium (b), B. subtilis (c), P. aeruginosa (d), P. vulgaris (e), V. cholerae (f),* and *C. albicans (g)* showed the maximum sensitivity to the AAG-NPs treatment. Zone of inhibition (h).

DLS particle size corresponded to the results obtained from XRD and TEM analyses. A previous study demonstrated that decreasing the particle size from 800 to 200 nm reduced phagocytosis.[28] The findings of this study demonstrated that the average size of the NPs was 148.30 nm, which subsides within the optimum range as determined by DLS analysis.

The morphological characteristics of the NPs were analyzed using SEM and TEM methods. The size of anti-tumor NPs is one of the parameters that affect their effectiveness. The EPR effect leads to the gathering of large molecules in the tumor microenvironment.[29,30] The size and morphology of the AAG-NPs were examined using SEM analysis, as depicted in Figure 3a. The microphotograph (Figure 3a) clearly shows that the AAG-NPs display hexagonal structures with varying aggregated appearances. The AAG-NPs have an average particle size of 55 to 70 nm. The observations validate the effective application of albumin and glutaraldehyde on the amygdalin surface matrix. The interactions observed can be due to the electrostatic forces between the components of the AAG-NPs surface matrix. Figure 3b displays an EDAX spectrum of the AAG-NPs. The primary elements present in the NPs were 56.86% of Copper (C), 16.67% of Nitrogen (N), 25.02% of Oxygen (O) and 1.45% of sulfur (S). This confirms the presence of these elements in the AAG-NPs.

The morphological and crystallographic structures of the AAG-NPs were investigated using TEM and SAED pattern analyses. These images demonstrate the production of AAG-NPs, which have spherical shapes. Significant aggregation was noted in the AAG-NPs, which may be due to the NP's elevated surface-area-to-volume ratio, which leads to a significant increase in surface energy (Figure 4A-E). The confirmation of

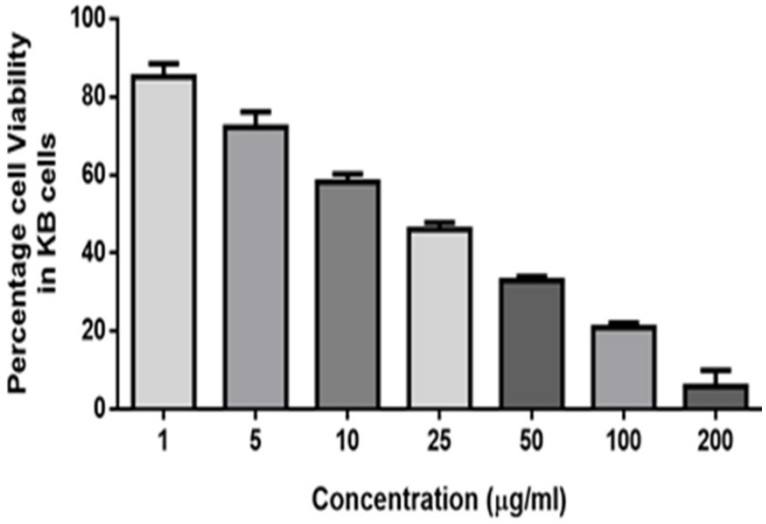

Figure 6: Effect of AAG-NPs on the viability of KB cells. The results indicate that the treatment of AAG-NPs at various concentrations (1, 5, 10, 25, 50, 100 and 200 µg/mL) significantly reduced the viability of KB cells. The IC_{50} level of AAG-NPs was found to be 23.97 µg/mL.

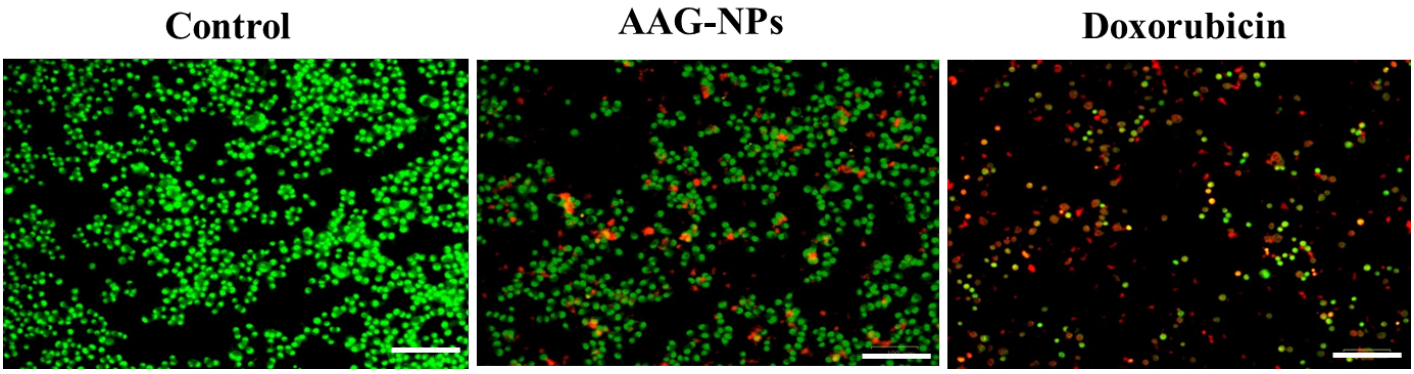

Figure 7: Effect of AAG-NPs on the apoptotic cell death in the KB cells. The IC_{50} concentration of 23.97 µg/mL of AAG-NPs treatment showed more cell membrane damage, nuclear shrinkage, a decrease in cell population and the presence of apoptotic bodies when compared with control, which confirms the onset of apoptosis. Positive control drug doxorubicin (10 µm) was used and the images were captured using a fluorescent microscope at 20 × magnification. Scale bar indicate 10 µm.

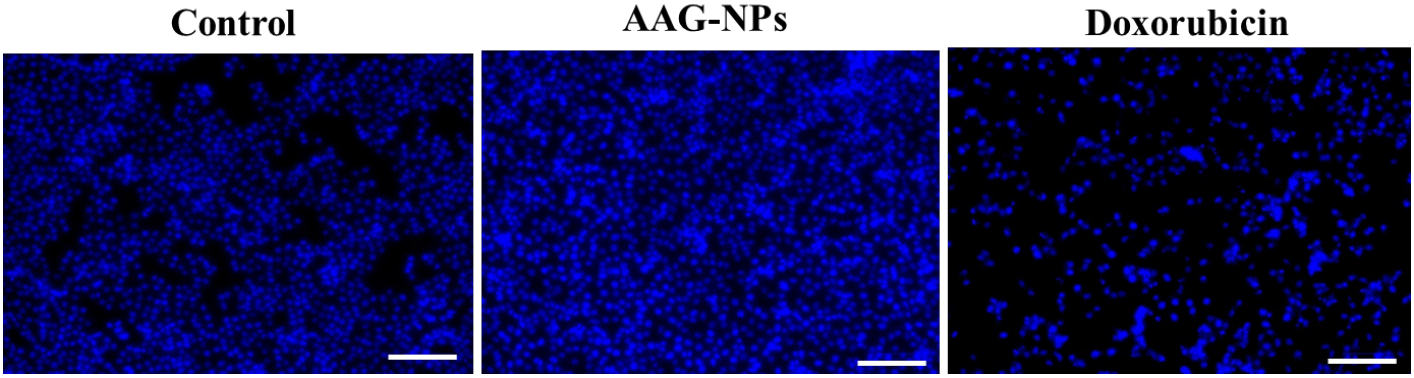

Figure 8: Effect of AAG-NPs on the apoptosis in the KB cells. The results showed that the treatment of KB cells with an IC_{50} concentration of 23.97 µg/mL of AAG-NPs resulted in increased apoptotic cell death and cell damage when compared with the control. Positive control drug doxorubicin (10 µm) was used and the images were captured using a fluorescent microscope at 20 × magnification. Scale bar indicate 10 µm.

the crystallization of the AAG-NPs was achieved through the analysis of the SAED patterns (Figure 4F).

The well diffusion technique was used to examine the antimicrobial properties of AAG-NPs against several pathogens, including *S. pneumoniae, B. megaterium, B. subtilis, P. aeruginosa, P. vulgaris, V. cholerae,* and *C. albicans* (Figure 5a-g). The use of various doses of NPs has shown notable antimicrobial efficacy against all examined pathogens. AAG-NPs effectively suppressed the growth of many pathogens, including *S. pneumoniae, P. aeruginosa*, and *C. albicans*. The increase in the zone area of inhibition noted around the wells treated with NPs serves as proof of the decreased growth of these pathogens (Figure 5h).

Carcinogenesis refers to the transformation of a normal, healthy cell into a cancer cell, a process that encompasses various genes and genetic alterations. Carcinogenesis is a complex mechanism that involves the initiation, promotion and development.[31] Rapid proliferation is a distinguishing characteristic of tumor cells, enabling them to overtake the growth of normal cells.

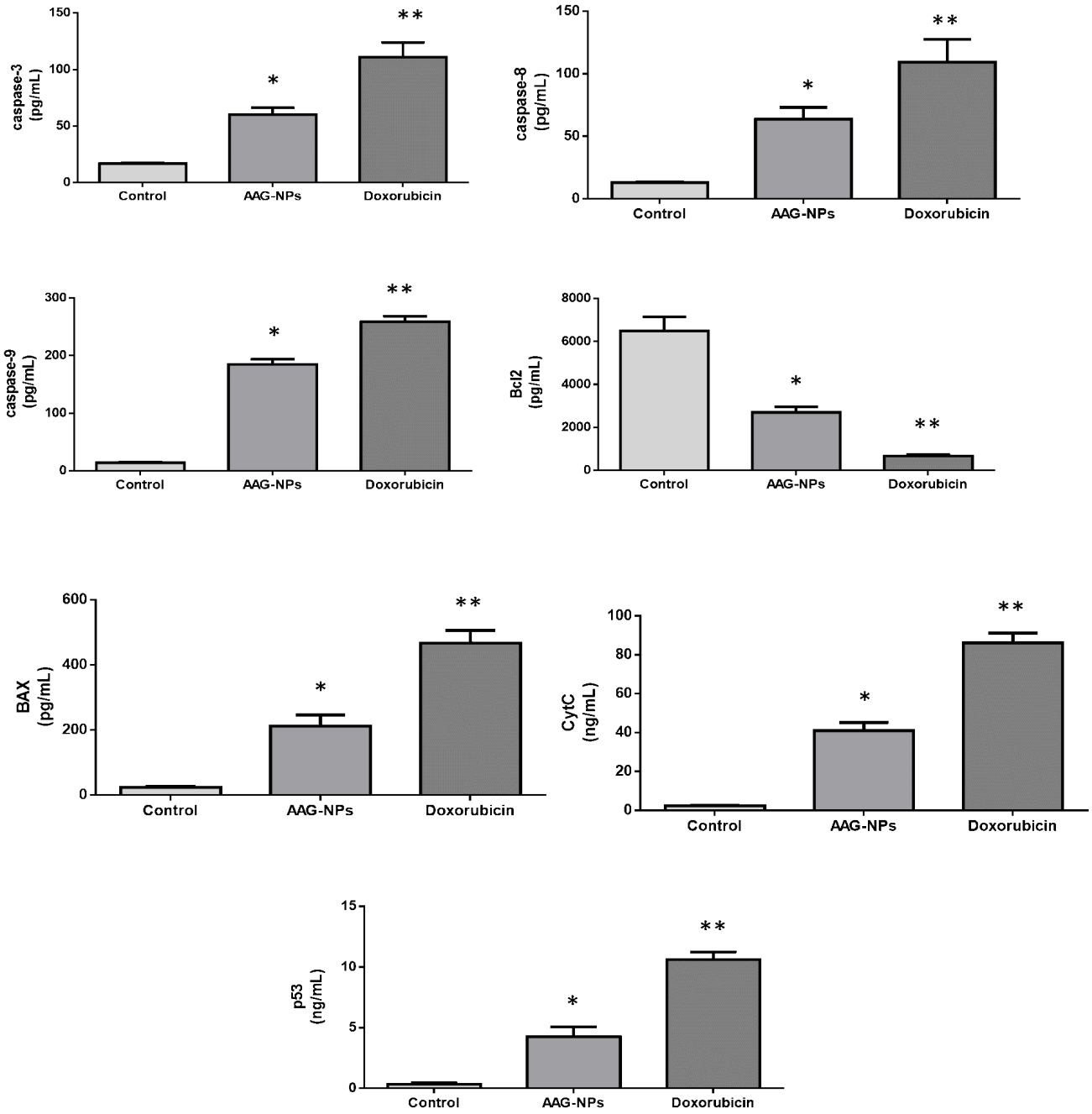

Figure 9: Effect of AAG-NPs on the apoptotic protein expressions in the KB cells. The data were analyzed using GraphPad Prism and depicted as a mean±SD of triplicate assays (n=3). One-way ANOVA and DMRT assays were used to analyze the data. The values do not share a common superscript and differ significantly (p<0.05) from the control group.

The major antitumor drugs are designed to specifically target rapidly dividing cells and inhibit, eliminate, or impede their proliferation. However, these anticancer drugs also have the adverse effect of damaging or annihilating healthy, non-cancerous cells. As a result, the patient will experience significant negative consequences and the therapy's efficacy will be restricted or reduced.[32] The current study aimed to evaluate the influence of AAG-NPs on the cell death of KB cells using the MTT assay. It is a well-established technique used to assess cytotoxicity following different treatments.[33] The results indicate that the treatment of AAG-NPs at various concentrations (1-200 µg/mL) remarkably decreased the growth of KB cells. The cell viability significantly decreased as the amounts of AAG-NPs increased compared to the untreated cells (Figure 6).

Apoptosis is a vital cellular mechanism that plays a crucial role in the growth, survival and functioning of cells. Therefore, the lack of regulation in the apoptotic process is frequently linked to a wide variety of diseases, more specifically cancer.[34,35] The findings of dual staining also proved that the apoptosis in the KB cells increased when treated with AAG-NPs at an IC_{50} dosage of 23.97 µg/mL (Figure 7). The intensity of yellow/orange fluorescence in the cells treated with AAG-NPs was higher than that of the control group (Figure 7), highlighting those AAG-NPs enhance apoptosis in KB cells. The treatment of 10 µM of doxorubicin also increased apoptotic cell death in KB cells, which supports the apoptotic-inducing potentials of the synthesized AAG-NPs.

Apoptosis-targeting drug candidates are extensively utilized in the treatment of cancer. These drugs induce significant alterations in the morphology and physiology of cancerous cells, including the formation of membrane blabbing, the condensation of the nucleus and the fragmentation of DNA.[36] In this study, the findings of both DAPI staining assays revealed that the synthesized AAG-NPs effectively induced apoptosis in KB cells, which supported its pro-apoptotic effects on oral cancer cells (Figure 8).

Apoptosis can occur through two distinct pathways: the mitochondrial pathway also referred to as the intrinsic pathway and the death receptor-mediated pathway, also known as the extrinsic pathway. Multiple proteins are involved in the apoptotic mechanism, such as caspases, Bax, Bcl-2 and p53 proteins. These proteins are crucial regulators of apoptosis.[37] It is well known that an important method by which NPs fight against cancer cells is by causing apoptosis, a process that activates caspases by increasing the Bax/Bcl-2 ratio and releasing Cyt-c from mitochondria.[38] The Bcl-2 gene is activated through a mechanism of chromosomal translocation in various cancers.[39] Bcl-2 suppresses apoptosis by preventing the Cyt-c release, hence inhibiting caspase activation.[40] Tumor cells have exhibited elevated Bcl-2 expression. The presence of Bcl-2 and mutant p53 in cancer cells may result in strong resistance to cisplatin and reduced chances of undergoing apoptosis.[41] An overexpression of Bcl-2 and a down-regulation of Bax result in a cellular homeostatic imbalance, ultimately leading to the development of cancer. Figure 9 exhibits the findings of an analysis of apoptotic protein expressions in the AAG-NPs-treated and control KB cells. Treatment with an IC_{50} concentration of AAG-NPs significantly increased the apoptotic protein expressions of Bax, Cyt-c, p53, caspase-3, -8 and -9, while reducing the Bcl-2 expression in KB cells.

The reduced Bax expression has been closely connected with various cancers and poor prognosis.[42] The study conducted by Camisasca[43] revealed that reduced Bax expression is connected with the advancement of oral cancer. A reduced level of Bax is linked to reduced cell death, progressed malignant tumors, poor prognosis, cancer development and resistance to chemotherapy in cancer patients.[44] In the current work, the findings proved that the AAG-NP treatment effectively increased apoptotic protein expression in the KB cells. Therefore, it was evident that AAG-NPs may induce apoptosis in KB cells by up-regulating apoptotic protein expression. 10 µM of doxorubicin also up-regulated the apoptotic protein expressions and reduced the Bcl-2 expression in the KB cells, which supports the apoptotic activity of AAG-NPs.

CONCLUSION

The current results demonstrate that AAG-NPs inhibit cellular proliferation and induce apoptosis in KB cells. AAG-NPs treatment induced apoptosis by increasing the Bax, p53, Cyt-c, caspase-3, -8 and -9 expressions while reducing the Bcl-2 expression in oral cancer KB cells. Hence, it can be talented AAG-NPs exhibit the potential to be a prospective therapeutic agent in the future. Nevertheless, further extensive analyses are still required to fully comprehend the various therapeutic roles of the AAG-NPs against cancer and other diseases.

ACKNOWLEDGEMENT

The authors extend their appreciation to the Researchers Supporting Project number (RSP-2024R98), King Saud University, Riyadh, Saudi Arabia for financial support.

FUNDING

The authors extend their appreciation to the Researchers supporting Project number (RSP-2024R98) at King Saud University, Riyadh, Saudi Arabia for financial support

CONFLICT OF INTEREST

The authors declare that there is no conflict of interest.

ABBREVIATIONS

pH: The potential of hydrogen; **M:** Molar; **mg:** Milligram; **µg:** Microgram; **GSH:** glutathione; **SOD:** Superoxide dismutase; **MDA:** Malondialdehyde; **CAT:** Catalase; **mL:** microliter; **IC_{50}:** Concentration of a compound with half-maximal cell viability;

DMSO: Dimethyl sulfoxide; **MMP:** Mitochondrial Membrane Potential (ΔΨm); **ROS:** Reactive Oxygen Species; **AO:** Acridine Orange; **XTT:** 2,3-bis[2-methoxy-4-nitro-5-sulfophenyl]-2H-tetr azolium-5-carboxanilide; **EtBr:** Ethidium Bromide; **CO_2:** Carbon dioxide; **DMEM:** Dulbecco's Modified Eagle Medium; **FBS:** Fetal Bovine Serum; **BAX:** BCL-2 associated X proteins; **BCL-2:** B cell lymphoma 2; **CRC:** Colorectal cancer; **ER:** Endoplasmic reticulum; **KRAS:** Kirsten rat sarcoma viral oncogene homolog; **5FU:** Fluorouracil; **DAPI:** 4',6-diamidino-2-phenylindole; **cm^2:** Square Centimeter; **PI:** Propidium Iodide; **PBS:** Phosphate buffer saline.

SUMMARY

Oral cancer, a type of head and neck cancer affecting the oral cavity and oropharynx, could benefit from advances in nanotechnology. This study explored the creation and anticancer potential of amygdalin-functionalized albumin-glutaraldehyde nanoparticles (AAG-NPs) against oral cancer KB cells. AAG-NPs were synthesized and characterized using various techniques, including UV-visible spectroscopy, X-ray diffraction and electron microscopy, revealing spherical particles averaging 148.30 nm in size. These nanoparticles exhibited significant antimicrobial properties against various pathogens and demonstrated strong cytotoxic effects on KB cells in MTT assays. Fluorescent staining assays confirmed apoptosis in treated KB cells, with increased expression of apoptotic proteins observed. The results suggest that AAG-NPs effectively inhibit KB cell proliferation and induce apoptosis, although further research is needed to fully elucidate the molecular mechanisms involved.

REFERENCES

1. Siegel R. L., Miller K. D., Jemal A. Cancer statistics, 2020. CA Cancer J. Clin. 2020;70(1):7-30.
2. Sung H., Ferlay J., Siegel R. L., Laversanne M., Soerjomataram I., Jemal A., *et al.* Global cancer statistics 2020: GLOBOCAN estimates of incidence and mortality worldwide for 36 cancers in 185 countries. CA Cancer J. Clin. 2021;71(3):209-49.
3. Mummudi N., Agarwal J.P., Chatterjee S., Mallick I., Ghosh-Laskar S. Oral Cavity Cancer in the Indian Subcontinent-Challenges and Opportunities. Clin. Oncol. R. Coll. Radiol. 2019;31:520-8.
4. Wessels R., De Roose S., De Bruyckere T., Eghbali A., Jacquet W., De Rouck T., *et al.* The Mucosal Scarring Index: Reliability of a new composite index for assessing scarring following oral surgery. Clin. Oral. Investig. 2019;23:1209-15.
5. Nandini D. B., Rao R. S., Hosmani J., Khan S., Patil S., Awan K. H. Novel therapies in the management of oral cancer: An update. Dis. Mon. 2020;66(12):101036.
6. Surer S. I., Elcitepe T. B., Akcay D., Daskin E., Calibasi Kocal G., Arican Alicikus Z., *et al.* A promising, novel radiosensitizer nanodrug complex for oral cavity cancer: Cetuximab and cisplatin-conjugated gold nanoparticles. Balk. Med. J. 2021;38(5):278-86.
7. Ketabat F., Pundir M., Mohabatpour F., Lobanova L., Koutsopoulos S., Hadjiiski L., *et al.* Controlled drug delivery systems for oral cancer treatment status and future perspectives. Pharmaceutics, 2019;11(7):302.
8. Sah A. K., Vyas A., Suresh P. K., Gidwani B. Application of nanocarrier-based drug delivery system in treatment of oral cancer. Artif. Cells Nanomed Biotechnol. 2018;46(4):650-7.
9. Dehelean C.A., Marcovici I., Soica C., Mioc M., Coricovac D., Iurciuc S., *et al.* Plant-Derived Anticancer Compounds as New Perspectives in Drug Discovery and Alternative Therapy. Molecules. 2021;26:1109.
10. Gavrilas L.I., Cruceriu D., Mocan A., Loghin F., Miere D., Balacescu O. Plant-Derived Bioactive Compounds in Colorectal Cancer: Insights from Combined Regimens with Conventional Chemotherapy to Overcome Drug-Resistance. Biomedicines. 2022;10: 1948.
11. Mohapatra P., Singh P., Singh D., Sahoo S., Sahoo S.K. Phytochemical Based Nanomedicine: A Panacea for Cancer Treatment, Present Status and Future Prospective. OpenNano. 2022;7:100055.
12. Edis Z., Wang J., Waqas M.K., Ijaz M., Ijaz M. Nanocarriers-Mediated Drug Delivery Systems for Anticancer Agents: An Overview and Perspectives. Int. J. Nanomed. 2021;16:1313-30.
13. Alhalmi A., Amin S., Khan Z., Beg S., Al kamaly O., Saleh A., *et al.* Nanostructured Lipid Carrier-Based Codelivery of Raloxifene and Naringin: Formulation, Optimization, *in vitro, ex vivo, in vivo* Assessment and Acute Toxicity Studies. Pharmaceutics. 2022;14:1771.
14. Arshi A., Hosseini S.M., Hosseini F.S.K., Amiri Z.Y., Hosseini F.S., Sheikholia Lavasani M., *et al.* The anti-cancer effect of amygdalin on human cancer cell lines. Mol. Biol. Rep. 2019;46:2059-66.
15. Qadir M., Fatima K. Review on Pharmacological Activity of Amygdalin. Arch. Cancer Res. 2017;5:10-12.
16. Baroni A., Paoletti I., Greco R., Satriano R.A., Ruocco E., Tufano M.A., *et al.* Immunomodulatory effects of a set of amygdalin analogues on human keratinocyte cells. Exp. Dermatol. 2005;14:854-859.
17. Al-Bakri S.A., Nima Z.A., Jabri R.R., Ajeel E.A. Antibacterial activity of apricot kernel extract containing Amygdalin. Iraqi J. Sci. 2010;51:571-6.
18. Guo J., Wu W., Sheng M., Yang S., Tan J. Amygdalin inhibits renal fibrosis in chronic kidney disease. Mol. Med. Rep. 2013;7:1453-7.
19. Yu C., Li L., Wang S., Xu Y., Wang L., Huang Y., *et al.* Advances in nanomaterials for the diagnosis and treatment of head and neck cancers: A review. Bioact. Mater. 2023;25:430-44.
20. Ding Z., Sigdel K., Yang L., Liu Y., Xuan M., Wang X., *et al.* Nanotechnology-based drug delivery systems for enhanced diagnosis and therapy of oral cancer. J. Mater. Chem. B. 2020;8:8781-93.
21. Rosenblum D., Joshi N., Tao W., Karp J.M., Peer D. Progress and challenges towards targeted delivery of cancer therapeutics. Nat. Commun. 2018;9:1410.
22. Lim S., Park J., Shim M.K., Um W., Yoon H.Y., Ryu J.H., *et al.* Recent advances and challenges of repurposing nanoparticle-based drug delivery systems to enhance cancer immunotherapy. Theranostics. 2019;9:7906-7923.
23. Virmani T., Kumar G., Virmani R., Sharma A., Pathak K. Nanocarrier-Based Approaches to Combat Chronic Obstructive Pulmonary Disease. Nanomedicine. 2022;17:1833-1854.
24. Zhang J., Lan C.Q., Post M., Simard B., Deslandes Y., Hsieh T.H. Design of nanoparticles as drug carriers for cancer therapy. Cancer Genom. Proteom. 2006;3:147-157.
25. Rahimizadeh P., Yang S., Lim S.I. Albumin: An Emerging Opportunity in Drug Delivery. Biotechnol. Bioprocess Eng. 2020;25:985-995.
26. Chen Q., Liu Z. Albumin Carriers for Cancer Theranostics: A Conventional Platform with New Promise. Adv. Mater. 2016;28:10557-66.
27. Yhee J.Y., Jeon S., Yoon H.Y., Shim M.K., Ko H., Min J., *et al.* Effects of tumor microenvironments on targeted delivery of glycol chitosan nanoparticles. J. Control. Release. 2017;267:223-31.
28. Langer K., Balthasar S., Vogel V., Dinauer N., Von Briesen H., Schubert D. Optimization of the preparation process for human serum albumin (HSA) nanoparticles. Int. J. Pharm. 2003;257:169-80.
29. Iyer A.K., Khaled G., Fang J., Maeda H. Exploiting the enhanced permeability and retention effect for tumor targeting. Drug Discov. Today. 2006;11:812-8.
30. Bolaños K., Kogan M.J., Araya E. Capping gold nanoparticles with albumin to improve their biomedical properties. Int. J. Nanomed. 2019;14:6387.
31. Chahar A., Chahar N., Kabirai A., Gupta J. Chemical Carcinogenesis: A Brief Review on Mechanism & Metabolism. J. Oral. Med. Oral Surg. Oral Pathol. Oral Radiol. 2020;6:120-4.
32. George B.P., Chandran R., Abrahamse H. Role of Phytochemicals in Cancer Chemoprevention: Insights. Antioxidants. 2021;10:1455.
33. Meerloo J.V., Kaspers G.J., Cloos J. Cancer Cell Culture. Springer; Berlin/Heidelberg, Germany: 2011. Cell sensitivity assays: The MTT assay; pp. 237-45.
34. Kaloni D, Diepstraten ST, Strasser A, Kelly GL. BCL-2 protein family: attractive targets for cancer therapy. Apoptosis. 2023;28(1-2):20-38.
35. Goldar S., Khaniani M.S., Derakhshan S.M., Baradaran B. Molecular mechanisms of apoptosis and roles in cancer development and treatment. Asian Pac. J. Cancer Prev. 2015;16:2129-44.
36. Pistritto G., Trisciuoglio D., Ceci C., Garufi A., D'Orazi G. Apoptosis as anticancer mechanism: Function and dysfunction of its modulators and targeted therapeutic strategies. Aging. 2016;8:603-19.
37. Strasser A, Harris AW, Huang DCS, Krammer PH, Cory S (1995) Bcl-2 and Fas/APO-1 regulate distinct pathways to lymphocyte apoptosis. EMBO J, 1995;14:6136-47.
38. Chen J., Zhang L., Hao M. Effect of artemisinin on proliferation and apoptosis-related protein expression *in vivo* and *in vitro*. Saudi J. Biol. Sci. 2018;25:1488-93.
39. Minn AJ, Velez P, Schendel SL, Liang H, Muchmore SW, Fesik SW, *et al.* Bcl-X(L) Forms an Ion Channel in Synthetic Lipid Membranes. Nature 1997;385:353-7.
40. Yin XM, Oltvai ZN, Korsmeyer SJ. BH1 and BH2 Domains of Bcl-2 are Required for Inhibition of Apoptosis and Heterodimerization With Bax. Nature 1994;369:321-3.

41. Han J-Y, Chung Y-J, Park SW, Kim JS, Rhyu M-G, Kim H-K, *et al.* The Relationship Between Cisplatin-Induced Apoptosis and P53, Bcl-2 and Bax Expression in Human Lung Cancer Cells. Korean J Intern Med (1999);14:42.
42. Jeong SH, Lee H-W, Han JH, Kang SY, Choi J-H, Jung YM, *et al.* Low Expression of Bax Predicts Poor Prognosis in Resected non-Small Cell Lung Cancer Patients With non-Squamous Histology. Jpn J Clin Oncol (2008);38:661-9.
43. Camisasca DR, Honorato J, Bernardo V, da Silva LE, da Fonseca EC, de Faria PA, *et al.* Expression of Bcl-2 Family Proteins and Associated Clinicopathologic Factors Predict Survival Outcome in Patients with Oral Squamous Cell Carcinoma. Oral Oncol (2009);45:225-33.
44. Nix P, Cawkwell L, Patmore H, Greenman J, Stafford N. Bcl-2 Expression Predicts Radiotherapy Failure in Laryngeal Cancer. Br J Cancer (2005);92:2185-9.

Cite this article: Munusamy MA, Sukumar K, Bharathi M, Alarfaj AA, Hussein-Al-Ali SH. An Albumin-Based Amygdalin-Glutaraldehyde Nanoparticle Induces Apoptosis in Oral Cancer KB Cells. Indian J of Pharmaceutical Education and Research. 2024;58(4s):s1271-s1281.